Pharmaceutical Research, Vol. 5, No. 5, 1988

Research Article

Dissolution of Ionizable Drugs in Buffered and Unbuffered Solutions

Sadettin S. Ozturk,[1,3] Bernhard O. Palsson,[1] and Jennifer B. Dressman[2]

Received September 9, 1987; accepted December 17, 1987

The dissolution kinetics of ionizable drugs (weak acids or bases) are analyzed with a mathematical model derived from the theory of mass transfer with chemical reaction. The model assumes that the overall process is diffusion limited, that all the reactions are reversible and instantaneous, and that dissolution and reaction are limited to the stagnant fluid film adjacent to the solid phase. Dissolution into buffered and unbuffered aqueous solutions are considered separately, with covenient analytical solutions obtained in both cases. In addition, equations for the time to partial and complete dissolution are derived. The dissolution rate is shown to be dependent on the pK_a and intrinsic solubility and the medium properties, i.e., pH, buffer capacity, and mass transfer coefficient. Equations of a form analogous to the nonionized case are derived to account explicitly for all these factors, with dissolution rates expressed in terms of the product of a driving force (concentration difference) and resistance (inverse of mass transfer coefficient). The solutions are in an accessible analytical form to calculate the surface pH and subsequently the surface concentrations driving the drug dissolution. Numerical examples to illustrate dissolution into unbuffered and buffered media are presented and the results are shown to be in accord with experimental data taken from the literature.

KEY WORDS: drug dissolution; ionization and dissolution; film model for dissolution; buffer effect on dissolution.

1. INTRODUCTION

It is of importance to both the formulator of pharmaceutical dosage forms and the pharmacy practitioner to understand clearly the fundamental factors affecting the rate of dissolution of drugs. In the case of drugs which do not ionize or otherwise react with the dissolution medium, dissolution can be predicted from available theory (1). In the film theory of mass transfer the dissolution rate, J, of a nonionized drug is expressed in terms of a driving force and a resistance, i.e.,

$$J = \frac{D}{\delta}(C_0 - C_b) = k_s \Delta C \qquad (1)$$

where C_0 and C_b are the intrinsic solubility of the drug and the concentration of drug in the bulk, D is the diffusion coefficient, δ is the diffusion layer thickness, and k_s is the mass transfer coefficient.[4] Provided that the mass transfer coefficient is known, all values in Eq. (1) can be obtained, enabling dissolution rates to be calculated. However, many drugs are weak acids or bases and undergo ionization when they dissolve. In these cases dissolution is accompanied by ionization reactions and consequently the intrinsic solubility is not an accurate representation of the concentration of drug at the dissolving surface. The simplest way to account for this is to express the dissolution rate in terms of a total solubility, C_T, defined as (2)

$$C_T = C_0\left(1 + \frac{K_a}{[H^+]}\right) \quad \text{and} \quad C_T = C_0\left(1 + \frac{[H^+]}{K_a}\right) \qquad (2)$$

for weak acids and weak bases, respectively, where K_a is the dissociation constant and $[H^+]$ is the hydrogen ion concentration. Total solubility, C_T, is then used in place of C_0 in Eq. (1). However, this approach assumes that the pH of the bulk and drug surface are identical, leading to discrepancies between predicted and observed dissolution rates. For instance, Shek (3) indicated that the dissolution rate and the total solubility calculated from the above equations do not show proportional behavior.

Mechanistic modeling of ionizable drug dissolution was initiated by Brunner by constructing a model for benzoic acid dissolution (4). Later Higuchi and coworkers (5,6) presented a detailed model that included the effect of buffer. A mass transfer with chemical reaction model was formulated to obtain simple expressions to describe the dissolution process. More recently Mooney and co-workers (7,8) and Aunins and co-workers (9) extended this analysis by devel-

[1] Department of Chemical Engineering, The University of Michigan, Ann Arbor, Michigan 48109.

[2] College of Pharmacy, The University of Michigan, Ann Arbor, Michigan 48109.

[3] To whom correspondence should be addressed.

[4] It should be noted that although this expression is commonly used in any geometry, it is derived only for a semiinfinite plane and care must be taken in its use. In spherical coordinates an additional term to account for the geometry appears in Eq. (1), viz, $(1 + \delta/R)$, with R being the radius.

0724-8741/88/0500-0272$06.00/0 © 1988 Plenum Publishing Corporation

oping expressions for weak acids in buffered and unbuffered aqueous solutions. Although their expressions provide a more comprehensive description of the dissolution process than earlier approaches, use of these expressions to obtain dissolution rates requires not only the driving force (concentration difference) of the drug but also those of the hydrogen ion, hydroxyl ion, and buffer.

Previous models therefore provide either approximate solutions for the dissolution rates with ionization or more complete solutions which are not easily applied. The objective of the current work is to provide a complete solution which mechanistically describes the dissolution of ionizable compounds and yet is of a form that is amenable for everyday application. The approach taken is essentially a refinement of the approach taken by Mooney and co-workers (7,8) modifying the setup of the boundary conditions at the surface in order to arrive at a system of equations that can be solved analytically, and the solution is of a form which permits easy calculation of dissolution under various conditions. The approach is to obtain an expression analogous to Eq. (1), in which the dissolution rate is expressed in terms of the concentration difference of the drug between the surface and the bulk. The effect of other species present on the concentration of drug at the surface must be accounted for in order to obtain a predictive expression for the dissolution rate.

The second objective is to model the fraction of drug dissolved at any given time. The dissolution time may be an important determinant of the rate and extent of drug absorption (2,10). Equations for "zero-order" release (11) and "cube root law" (12) are available for nonionized drug dissolution but for the case of ionizable drugs no similar analysis has been reported. Once a predictive dissolution rate expression is established, the decrease in the particle size and, subsequently, the amount of drug dissolved at a given time can be calculated.

2. MATHEMATICAL DESCRIPTION OF THE DISSOLUTION PROCESS

2.1. General Mass Transfer Equations

When an ionizable drug is exposed to an aqueous phase with or without buffer it diffuses out of the solid phase and dissolves and reacts with water (hydroxyl or hydrogen ion) and/or buffer (base or acid conjugate). Figure 1 illustrates the dissolution of a weak acid in buffered medium as an example. Since several ions are present in the medium, other ionic reactions also take place simultaneously.

A complete description of mass transfer for this mixture of reactive species requires consideration of the contributions of diffusion, convection, and reaction. By using Fick's law for diffusion the general mass balance for a given species takes the form (13)

$$\frac{\partial C_i}{\partial t} + \mathbf{v} \cdot \nabla C_i = D_i \nabla^2 C_i + \sum_k \nu_{i,k} \phi_k \qquad (3)$$

where for species i, C_i is the molar concentration, D_i is the diffusion coefficient, ∇C_i is the concentration gradient, and $\nabla^2 C_i$ is the Laplacian of concentration. The kth reaction rate is ϕ_k, $\nu_{i,k}$ is the stoichiometric coefficient of component i in the kth reaction (positive for products, negative for reactants), v is the fluid velocity vector, and t is time.

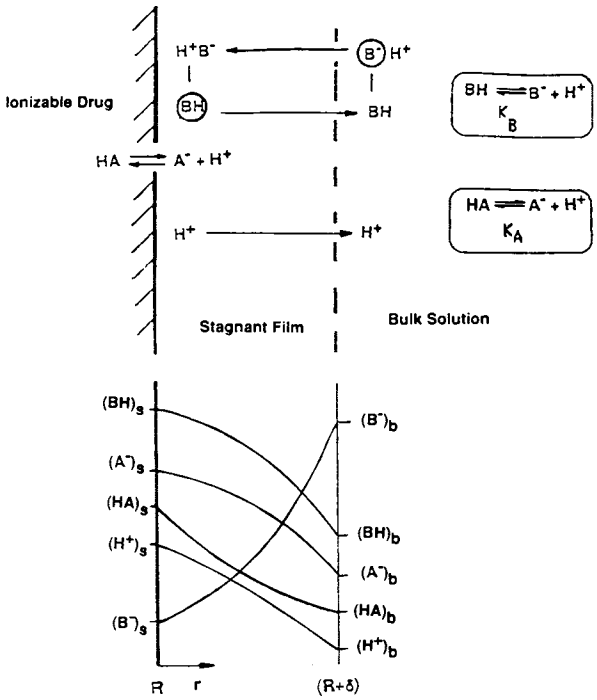

Fig. 1. Schematic representation of dissolution process and concentration profiles in dissolution of a weak acid-type drug, HA, in buffer solution, HB.

2.2. Simplifying Assumptions

The description given by Eq. (3) is general but simplifying assumptions can be made for the specific situations of interest.

2.2.1. Convection. If the bulk solution is a well-mixed homogeneous mixture with no concentration gradients, then we can assume that all the processes are confined into a stagnant film around the solid; hence the term $\mathbf{v} \cdot \nabla C_i$ disappears. This idealization is the standard stagnant film model for analyzing mass transfer processes.

2.2.2. Quasi-Steady-State Assumptions. The overall process that is of importance here is the dissolution of the solid drug core. If the transient behavior of the concentrations in the surrounding film is rapid, relative to the dissolution process, then we can assume that a steady-state concentration profile in the film is established instantly. Mathematically this amounts to removing the unsteady-state term, $\partial C_i/\partial t$, from the equations and writing

$$D_i \nabla^2 C_i + \Sigma \nu_{i,k} \phi_k = 0 \qquad (4)$$

This assumption is reasonable since in practice, the film thickness is of the order of 100 μm and the diffusional response time with a diffusivity value of 10^{-5} is approximately $t_{\text{diff}} = \delta^2/D \simeq (0.01\ \text{cm})^2/10^{-5}\ \text{cm}^2/\text{sec} = 10$ sec, which is very small compared to most dissolution times of interest. A more detailed discussion of diffusional transients is given by Crank (14), and their use for model simplification by Palsson (15).

2.2.3. Idealized Geometry. We will approximate the shape of a drug tablet as a sphere with concentration gra-

dients only in the radical direction. In these circumstances, the Laplacian operator for spherical coordinates can be introduced into Eq. (4) to give

$$\frac{D_i}{r^2}\frac{d}{dr}\left(r^2\frac{dC_i}{dr}\right) + \sum \nu_{i,k}\phi_k = 0 \qquad (5)$$

The general results presented in this paper are independent of the geometry choosen. Extensive discussion of the specific effects of geometry can be found in the literature (16).

The two cases of interest, i.e., dissolution into buffered or unbuffered media, are treated separately in Sections 3 and 4. First we discuss the appropriate boundary conditions for Eq. (5) and apply a moving-boundary approach to the mathematical description of the dissolution process.

2.3. Boundary Conditions

Since the governing equation, Eq. (5), is second order we need to specify two boundary conditions for each species. A convenient choice is to use the conditions at the solid drug surface and in the bulk of the dissolution medium.

2.3.1. Solid Drug Surface. The solid phase is assumed to consist of compacted solid drug such that the solid/liquid interface is open only to the dissolving species (nonionized form). The diffusivity of small molecules such as water, hydrogen ions, and buffer in solid diffusion media would be about four orders of magnitude lower than in aqueous solution (10^{-10} vs 10^{-6} cm^2/sec) so the fluxes into the solid drug per se can be considered negligible. We must also assume that there is relatively little infiltration of water, and subsequently other soluble species, along channels in the solid phase. If this assumption were violated, the change in surface area with time would not be adequately described by the model. For the nonpenetrating species we have

$$J_i = -D_i\frac{dC_i}{dr} = 0 \quad \text{or} \quad \frac{dC_i}{dr} = 0$$

for $i = 1, 2, \ldots, n$, $i \neq$ nononized drug species (6)

The concentration of nonionized drug at the surface is simply

$$C_{drug} = C_s = C_0 \qquad (7)$$

where C_0 is the intrinsic solubility, a known value.

2.3.2. Bulk. The bulk is assumed to be well mixed. Under these conditions we have

$$C_i = C_{i,b} \qquad \text{for } i = 1, 2, \ldots, n \qquad (8)$$

which are measurable values for each species.

These boundary conditions differ from those used in previous analyses (5–8) which require material balances in the diffusional layer. It will be seen later (Section 5) that the boundary conditions we have chosen allow us to obtain convenient expressions for the dissolution rates.

2.4. Dissolution Rates and the Moving-Boundary Equation

As the dissolution of drug proceeds, the solid phase erodes and the particle size decreases. The use of the quasi-steady-state approximation simplifies the analysis considerably since the transients considered are only those of the dissolution process.

The dissolution process can be described by a transient macroscopic mass balance on the drug as

$$-\frac{dn}{dt} = (\text{area})(\text{dissolution flux}) = (4\pi R^2)(J) \qquad (9)$$

where n is the number of moles of the drug species in the drug phase and R is the radius. If the particle radius R and dissolution flux J (rate per unit area) are relatively constant, then integration of this equation results in the well-known "zero-order" release:

$$n_0 - n = (4\pi R^2)Jt = kt \qquad (10)$$

This simplification does not apply to the system described here, since the particle size diminishes as the dissolution proceeds. We can account for the changes in the particle size by introducing the solid drug volume, and consequently the radius, as

$$n = \rho_M\left(\frac{4}{3}\pi R^3\right) \qquad (11)$$

where ρ_M is the molal density. Introducing Eq. (11) into Eq. (9) we get

$$-\rho_M\frac{dR}{dt} = J \qquad (12)$$

We will use Eq. (12) to describe the variation in the particle radius. The flux of the solid drug from the surface will be denoted by J, and once we obtain the expression for J (Section 5.1) we will introduce it into Eq. (12). The resulting equation can be integrated to give an expression for the radius in terms of time and hence the partial and total dissolution times (Section 5.2).

3. DISSOLUTION INTO UNBUFFERED MEDIA

3.1. Case 1. Weak Acid Dissolution

3.1.1. The Reaction Structure. The concentration of HA at the solid–fluid interface is $[HA]_0$, the intrinsic solubility. The drug molecule diffuses from the solid–fluid interface and is simultaneously ionized to give conjugate base A^- and H^+. The bulk at the end of the film is assumed to be well mixed, and furthermore the equilibria are attained throughout. The ionization reactions presented in Fig. 1 are[5]

$$HA \rightleftharpoons A^- + H^+$$
$$H_2O \rightleftharpoons OH^- + H^+$$
$$HA + OH^- \rightleftharpoons A^- + H_2O$$

They can be represented in a matrix notation as

$$\begin{pmatrix} -1 & 1 & 1 & 0 & 0 \\ 0 & 0 & 1 & 1 & -1 \\ -1 & 1 & 0 & -1 & 1 \end{pmatrix} \begin{pmatrix} HA \\ A^- \\ H^+ \\ OH^- \\ H_2O \end{pmatrix} = AC = 0 \qquad (13)$$

[5] The analysis presented in the paper assumed infinite solubility for all the ionic species. A limited solubility for an ionic species would require consideration of one more reaction, precipitation: $X^-_{aq} + M^+_{aq} \rightleftharpoons MX_s$.

Where A is a matrix of stoichiometric coefficients and C is a (5 × 1) concentration vector. The rank of A is 2 and therefore only two of the reactions are independent (17). We choose

$$\phi_1 \quad HA \rightleftharpoons A^- + H^+ \quad K_a = [A^-][H^+]/[HA]$$
$$\phi_2 \quad H_2O \rightleftharpoons OH^- + H^+ \quad K_w = [OH^-][H^+]$$

as our two independent reactions.

3.1.2. Mass Balances and Boundary Conditions. Introducing the two reaction rates leads to the following mass balance equations:

$$\frac{D_{HA}}{r^2}\frac{d}{dr}\left(r^2\frac{d[HA]}{dr}\right) = \phi_1 \tag{14}$$

$$\frac{D_{A^-}}{r^2}\frac{d}{dr}\left(r^2\frac{d[A^-]}{dr}\right) = -\phi_1 \tag{15}$$

$$\frac{D_{H^+}}{r^2}\frac{d}{dr}\left(r^2\frac{d[H^+]}{dr}\right) = -\phi_2 - \phi_1 \tag{16}$$

$$\frac{D_{OH^-}}{r^2}\frac{d}{dr}\left(r^2\frac{d[OH^-]}{dr}\right) = -\phi_2 \tag{17}$$

The boundary conditions that accompany these equations are as follows:

(i) at the surface, $r = R$,

$$[HA] = [HA]_s = [HA]_0 \tag{18}$$

and

$$\frac{d[A^-]}{dr} = \frac{d[H^+]}{dr} = \frac{d[OH^-]}{dr} = 0 \tag{19}$$

(ii) at the bulk edge of the diffusion layer, $r = R + \delta$,

$$[X] = [X]_b \tag{20}$$

where X represents HA, A^-, OH^-, and H^+, all of which are measurable bulk concentrations. In many cases of interest the bulk concentration of dissolving drug $[HA]_b$ and $[A^-]_b$ can be approximated to zero (sink conditions).

The flux of drug species is given by

$$J_{HA} = -D_{HA}\left(\frac{d[HA]}{dr}\right)_{r=R} \tag{21}$$

The next objective is to obtain an expression for J_{HA}.

3.1.3. Solution of the Differential Equations. Since the reaction rates ϕ_i are not known, we cannot integrate Eqs. (14)–(17) directly to get the solutions for the concentration of individual species. However the ϕ_i's can be eliminated by forming appropriate combinations of Eqs. (14)–(17). Adding Eq. (14) and Eq. (15) gives

$$\frac{1}{r^2}\frac{d}{dr}\left[r^2\frac{d}{dr}(D_{HA}[HA] + D_{A^-}[A^-])\right] = 0 \tag{22}$$

which can be integrated twice to give

$$D_{HA}[HA] + D_{A^-}[A^-] = D_{HA}([HA] + \gamma_{HA}[A^-]) = D_{HA}[HA]_T = C_1 + (C_2/r) \tag{23}$$

where C_1 and C_2 are the integration constants (see Table I). We define the "dynamic total concentration of drug" as $[HA]_T = [HA] + \gamma_{HA}[A^-]$, with $\gamma_{HA} = D_{A^-}/D_{HA}$.

Similarly, subtracting Eqs. (15) and (17) from Eq. (16) gives

$$\frac{1}{r^2}\frac{d}{dr}\left[r^2\frac{d}{dr}(D_{H^+}[H^+] - D_{OH^-}[OH^-] - D_{A^-}[A^-])\right] = 0 \tag{24}$$

and

$$D_{H^+}[H^+] - D_{OH^-}[OH^-] - D_{A^-}[A^-] = C_3 + (C_4/r) \tag{25}$$

Again, C_3 and C_4 are constants of integration (see Table I).

3.1.4. Determination of the Surface pH. The surface pH is very important, as it determines the concentration of all the other species through the equlibirium constants. Furthermore, we show in Section 5 that the dissolution rate can be calculated from these concentrations. This eliminates the need for the tedious calculation of the concentration profiles. At the surface we know the intrinsic solubility of drug, $[HA]_0$, so we can write

$$[A^-]_s = \frac{K_a[HA]_0}{[H^+]_s} \quad \text{and} \quad [OH^-]_s = \frac{K_w}{[H^+]_s} \tag{26}$$

Using the above expressions in Eq. (25) with constants C_3 and C_4, we obtain an equation for the H^+ concentration in terms of the bulk concentrations and drug intrinsic solubility.

$$D_{H^+}[H^+]_s - D_{OH^-}\frac{K_w}{[H^+]_s} - D_{A^-}\frac{K_a[HA]_0}{[H^+]_s} = D_{H^+}[H^+]_b - D_{OH^-}[OH^-]_b - D_{A^-}[A^-]_b \tag{27}$$

Table I. Integration Constants of Differential Equations for Acidic Drug

	Unbuffered medium [Eqs. (23) and (25)]	Buffered medium [Eqs. (38)–(40)]
C_1	$-D_{HA}\left[[HA]_{T,s}\frac{R}{\delta} - [HA]_{T,b}\left(\frac{R}{\delta}+1\right)\right]$	$-D_{HA}\left[[HA]_{T,s}\frac{R}{\delta} - [HA]_{T,b}\left(\frac{R}{\delta}+1\right)\right]$
C_2	$D_{HA}([HA]_{T,s} - [HA]_{T,b})R\left(\frac{R}{\delta}+1\right)$	$D_{HA}([HA]_{T,b} - [HA]_{T,s})R\left(\frac{R}{\delta}+1\right)$
C_3	$D_{H^+}[H^+]_b - D_{OH^-}[OH^-]_b - D_{A^-}[A^-]_b$	$D_{HB}[HB]_{T,b}$
C_4	0	0
C_5		$D_{H^+}[H^+]_b - D_{OH^-}[OH^-]_b - D_{A^-}[A^-]_b - D_{B^-}[B^-]_b$
C_6		0

Rearrangement of this expression gives a simple quadratic equation in $[H^+]_s$ whose physically meaningful root is given by $[H^+]_s = (-b + \sqrt{b^2 + 4c})/2$ (see Table II for constants). Once the $[H^+]_s$ value is known the other concentrations ($[A^-]_s$, $[OH^-]_s$) are obtained from Eq. (26). Calculation of the surface concentration for benzoic acid dissolution illustrates the use of this analysis (see the Appendix).

3.2. Case 2. Weak Base Dissolution

An analogous treatment for basic drugs gives a quadratic expression for the surface pH whose physically meaningful root is given by $[H^+]_s = (-b + \sqrt{b^2 + 4ac})/2a$ (see Table II). Once the $[H^+]_s$ value is known the other concentrations ($[BsH^+]_s$, $[OH^-]_s$) can easily be obtained from the appropriate equilibrium relationships and the calculation of surface concentrations is readily carried out. As an example, calculations for papaverine dissolution at bulk pH 2 are presented in the Appendix.

4. DISSOLUTION OF WEAK ACIDS IN THE PRESENCE OF BUFFER

The solution procedure for dissolution of weak acids in buffered media is similar to, but more complex than, the unbuffered case and is comprised of four solution steps.

4.1. The Reaction Structure

When an ionizable drug is exposed to a buffer solution it dissolves and reacts with the hydroxyl ion of the water or the base conjugate of the buffer and diffuses out of the solid phase. Figure 1 is a pictorial representation of the concentration profiles in the stagnant diffusional film during the dissolution of a weak acid HA in buffer solution. The reactions are

$$\begin{pmatrix} 0 & 0 & 0 & 0 & 1 & 1 & -1 \\ -1 & 1 & 0 & 0 & 1 & 0 & 0 \\ -1 & 1 & 0 & 0 & 0 & -1 & 1 \\ -1 & 1 & -1 & 1 & 0 & 0 & 0 \\ 0 & 0 & 1 & -1 & 0 & -1 & 1 \end{pmatrix} \begin{pmatrix} HA \\ A^- \\ B^- \\ BH \\ H^+ \\ OH^- \\ H_2O \end{pmatrix} = AC = 0 \quad (28)$$

Since the stoichiometric coefficient matrix, A, has a rank of 3, we have three independent reactions. Here we choose

ϕ_1 $HA \rightleftharpoons A^- + H^+$ $K_a = [A^-][H^+]/[HA]$
ϕ_2 $HB \rightleftharpoons B^- + H^+$ $K_b = [B^-][H^+]/[HB]$
ϕ_3 $H_2O \rightleftharpoons OH^- + H^+$ $K_w = [OH^-][H^+]$

4.2. Mass Balances and Boundary Conditions

The following balance equations are written by introducing the reaction rates:

$$\frac{D_{HA}}{r^2}\frac{d}{dr}\left(r^2\frac{d[HA]}{dr}\right) = \phi_1 \quad (29)$$

$$\frac{D_{A^-}}{r^2}\frac{d}{dr}\left(r^2\frac{d[A^-]}{dr}\right) = -\phi_1 \quad (30)$$

$$\frac{D_{B^-}}{r^2}\frac{d}{dr}\left(r^2\frac{d[B^-]}{dr}\right) = -\phi_2 \quad (31)$$

$$\frac{D_{HB}}{r^2}\frac{d}{dr}\left(r^2\frac{d[HB]}{dr}\right) = \phi_2 \quad (32)$$

$$\frac{D_{H^+}}{r^2}\frac{d}{dr}\left(r^2\frac{d[H^+]}{dr}\right) = -\phi_1 - \phi_2 - \phi_3 \quad (33)$$

$$\frac{D_{OH^-}}{r^2}\frac{d}{dr}\left(r^2\frac{d[OH^-]}{dr}\right) = -\phi_3 \quad (34)$$

The boundary conditions are as follows:
(i) at $r = R$, surface

$$[HA] = [HA]_s = [HA]_0 \quad (35)$$

and

$$\frac{d[A^-]}{dr} = \frac{d[B^-]}{dr} = \frac{d[HB]}{dr} = \frac{d[H^+]}{dr} = \frac{d[OH^-]}{dr} = 0 \quad (36)$$

(ii) at $r = R + \delta$, i.e., the bulk edge of the diffusion layer,

$$[X] = [X]_b \quad (37)$$

where X is HA, A^-, B^-, HB, OH^-, and H^+.

4.3. Solution of the Differential Equations

As before, appropriate combinations of the differential equations permit elimination of unknown reaction terms, ϕ_i.
(i) Addition of Eqs. (29) and (30) leads to

$$D_{HA}[HA] + D_{A^-}[A^-] = D_{HA}([HA] + \gamma_{HA}[A^-]) = D_{HA}[HA]_T = C_1 + (C_2/r) \quad (38)$$

Here we define, as before, the dynamic total concentration of drug $[HA]_T = [HA] + \gamma_{HA}[A^-]$, with $\gamma_{HA} = D_{A^-}/D_{HA}$.

Table II. Equation for Surface pH Calculation and Related Constants (Unbuffered Medium)

	Acidic drug	Basic drug
$[H^+]_s$	$(-b + \sqrt{b^2 + 4c})/2$	$(-b + \sqrt{b^2 + 4ac})/2a$
a		$K_a + \gamma_2[B_s]_0$
b	$-[H^+]_b + \gamma_1[OH^-]_b + \gamma_2[A^-]_b$	$(-[H^+]_b + \gamma_1[OH^-]_b - \gamma_2[BsH^+]_b)K_a$
c	$\gamma_1 K_w + \gamma_2 K_a[HA]_0$	$\gamma_1 K_w K_a$
γ_1	D_{OH^-}/D_{H^+}	D_{OH^-}/D_{H^+}
γ_2	D_{A^-}/D_{H^+}	D_{BsH^+}/D_{H^+}

(ii) Addition of Eqs. (31) and (32) leads to

$$D_B\text{-}[B^-] + D_{HB}[HB] = D_{HB}([HB] + \gamma_{HB}[B^-]) = D_{HB}[HB]_T = C_3 + (C_4/r) \quad (39)$$

where we have defined the "dynamic total buffer concentration" $[HB]_T = [HB] + \gamma_{HB}[B^-]$, with $\gamma_{HB} = D_B\text{-}/D_{HB}$.

(iii) From Eqs. (33), (34), (30), and (31),

$$D_{H^+}[H^+] - D_{OH^-}[OH^-] - D_A\text{-}[A^-] - D_B\text{-}[B^-] = C_5 + (C_6/r) \quad (40)$$

The constants of integration are found by applying boundary conditions, and are given in Table I.

4.4. Determination of the Surface pH

As for the unbuffered case, once the surface pH, $(pH)_s$, is known, the concentration of the other species can be determined. At the surface the concentration of HA is known to be $[HA]_0$ and we can solve the following equations:

$$[A^-]_s = \frac{K_a[HA]_s}{[H^+]_s} = \frac{K_a[HA]_0}{[H^+]_s} \quad (41)$$

$$[B^-]_s = \frac{K_b[HB]_{T,s}}{\gamma_{HB}K_b + [H^+]_s} = \frac{K_b[HB]_{T,b}}{\gamma_{HB}K_b + [H^+]_s} \quad (42)$$

$$[OH^-]_s = \frac{K_w}{[H^+]_s} \quad (43)$$

Using the above expressions in Eq. (40) we get

$$D_{H^+}[H^+]_s - D_{OH^-}\frac{K_w}{[H^+]_s} - D_A\text{-}\frac{K_a[HA]_0}{[H^+]_s} - D_B\text{-}\frac{K_b[HB]_{T,b}}{\gamma_{HB}K_b + [H^+]_s} = D_{H^+}[H^+]_b - D_{OH^-}(OH)_b - D_A\text{-}[A^-]_b - D_B\text{-}[B^-]_b \quad (44)$$

After rearrangement we get a cubic equation for $[H^+]_s$ whose physically meaningful root is $[H^+]_s = 2\sqrt{-Q}\cos(\theta/3) - a/3$ (see Table III). Calculations for 2-naphthoic acid in imidazole base buffer at pH 9 are provided as an example in the Appendix.

A similar treatment for weak base dissolution leads to an analogous cubic equation (Table III). The above derivations apply to dissolution into monoprotic buffers. Aunins and co-workers (9) have derived equations to describe dissolution into polyprotic buffers and expressions similar to theirs would be obtained for surface pH if the current approach was taken. However, the expression for dissolution rate would be simpler and of a form identical to Eq. (45) (see below).

5. CALCULATION OF THE DISSOLUTION RATE

5.1. Dissolution Fluxes

Using the solutions to the differential equations for both the unbuffered and the buffered conditions, we can obtain an expression for the dissolution rate. For the case of weak acids, the flux is defined by Eq. (21) and a concentration profile for HA is needed. The solution method, however, provides a simple expression only for the "dynamic total concentration of drug," $[HA]_T$ [Eq. (23) or (38)], and not for HA. This difficulty is overcome by the use of boundary conditions at the surface. Starting from the definition of J_{HA}

$$J_{HA} = -D_{HA}\left(\frac{d[HA]}{dr}\right)_{r=R} = -D_{HA}\left[\left(\frac{d[HA]_T}{dr}\right)_{r=R} - \gamma_{HA}\left(\frac{d[A^-]}{dr}\right)_{r=R}\right]$$

and recognizing that $d[A^-]/dr$ is zero at the surface, we obtain

$$J_{HA} = -D_{HA}\left(\frac{d[HA]_T}{dr}\right)_{r=R} = \frac{D_{HA}}{\delta}([HA]_{T,s} - [HA]_{T,b})\left(1 + \frac{\delta}{R}\right)$$

An analogous expression is obtained for weak bases:

$$J_{Bs} = \frac{D_{Bs}}{\delta}([Bs]_{T,s} - [Bs]_{T,b})\left(1 + \frac{\delta}{R}\right)$$

Both these flux expressions are of the form

$$J = \frac{D}{\delta}[(C)_{T,s} - (C)_{T,b}]\left(1 + \frac{\delta}{R}\right) \quad (45)$$

Table III. Equation for Surface pH Calculation and Related Constants (Buffered Medium)

	Acidic drug	Basic drug
$[H^+]_s$	$2\sqrt{-Q}\cos(\theta/3) - a/3$	$2\sqrt{-Q}\cos(\theta/3) - a/3$
Q	$(3b - a^2)/9$	$(3b - a^2)/9$
R	$(9ab - 27c - 2a^3)/54$	$(9ab - 27c - 2a^3)/54$
θ	$\cos^{-1}(R/\sqrt{Q^3})$	$\cos^{-1}(R/\sqrt{Q^3})$
a	$\gamma_{HB}K_b - G$	$(\gamma_{HB}K_aK_b + \gamma_2[Bs]_0K_b - GK_a)/(K_a + \gamma_2[Bs]_0)$
b	$-(\gamma_1K_w + \gamma_2K_a[HA]_0 + \gamma_3K_b[HB]_{T,b} + G\gamma_{HB}K_b)$	$-(\gamma_1K_aK_w + \gamma_3[HB]_{T,b}K_aK_b + \gamma_{HB}GK_aK_b)/(K_a + \gamma_2[B_s]_0)$
c	$-(\gamma_1K_w + \gamma_2K_a[HA]_0)\gamma_{HB}K_b$	$-\gamma_1\gamma_{HB}K_wK_aK_b/(K_a + \gamma_2[B_s]_0)$
G	$[H^+]_b - \gamma_1[OH^-]_b - \gamma_2[A^-]_b - \gamma_3[B^-]_b$	$[H^+]_b - \gamma_1[OH^-]_b + \gamma_2[BsH^+]_b - \gamma_3[B^-]_b$
γ_1	D_{OH^-}/D_{H^+}	D_{OH^-}/D_{H^+}
γ_2	D_{A^-}/D_{H^+}	D_{BsH^+}/D_{H^+}
γ_3	D_{B^-}/D_{H^+}	D_{B^-}/D_{H^+}

where $(C)_{T,s}$ and $(C)_{T,b}$ are the dynamic total surface and bulk concentrations of the drug, respectively. This expression is analogous to the one for nonionizable drugs, Eq. (1), with the geometrical term $[1 + (\delta/R)]$ included (see footnote 4). As for the nonionized case the dissolution rate is governed by the concentration difference between the drug surface and the bulk (driving force) and a mass transfer coefficient. The difference between the two expressions is that for the case of an ionizable compound, $[HA]_{T,s}$ must be calculated based on the surface pH, which in turn will vary with the bulk pH and buffer concentration as well as the drug solubility and pK_a.

5.2. Time for Complete Dissolution

After obtaining the expression for the dissolution rate we can integrate Eq. (12) to give the thickness of the moving boundary, i.e., the size of the solid phase. If the total concentration of drug in the bulk is zero (sink condition), then the dissolution rate is given by

$$J = \frac{D}{\delta}(C)_{T,s}\left(1 + \frac{\delta}{R}\right) = k_s(C)_{T,s}\left(1 + \frac{\delta}{R}\right) \qquad (46)$$

Introduction of Eq. (46) into the moving-boundary equation, followed by integration between $t = 0$ ($R = R_0$ and $t = t(R = R)$ (assuming that k_s is a constant), gives

$$t = \rho_M \frac{(R_0 - R) - \delta \ln[(R_0 + \delta)/(R + \delta)]}{k_s(C)_{T,s}} \qquad (47)$$

In light of the available evidence in the literature (18) the assumption of a constant mass transfer coefficient, or film thickness, is reasonable.

The time for complete dissolution t_c is the time at which $R = 0$ and can directly be obtained from the equations above:

$$t_c = \rho_M \frac{R_0 - \delta \ln(1 + R_0/\delta)}{k_s(C)_{T,s}} \qquad (48)$$

Note that application of this equation to the calculation of dissolution time requires that the mass transfer coefficient, k_s, must be measured or estimated for the system of interest.

5.3. The "Thin" Film Approximation

An important limit is when $\delta \ll R$. This corresponds to the case when either the film thickness is small and the curvature is negligible or we approach slab geometry. The latter case is important for analysis of rotating-disk experiments. In this limit the term $(1 + \delta/R)$ becomes unity and the mass release can be accounted for using the following equation, which has a form analogous to the cube root law for dissolution of nonionizable drug.

$$m^{1/3} = m_0^{1/3} - bt \quad \text{with} \quad b = \left(\frac{3\pi\rho}{4}\right)^{1/3} \frac{k_s(C)_{T,s}}{\rho_M} \qquad (49)$$

The equations for the dissolution rates in a rotating-disk apparatus are formulated in a rectangular coordinate system. Our analysis can be applied to the rotating-disk case by considering that the curvature radius is infinite. For a rotating disk the film thickness is explicitly expressed in terms of the rotating speed (19):

$$\delta = 1.612 D^{1/3} \nu^{1/6} \omega^{-1/2} \qquad (50)$$

where D is the diffusivity of the dissolving species, ν is the kinematic viscosity, and ω is the angular velocity in radians per unit time. Using this film thickness, δ in our results we can calculate the dissolution rates for a rotating disk. The value of $[H^+]_s$ is obtained from the procedure given in Sections 3.1.4 and 4.4, and by using this to calculate the value of $(C)_{T,s}$, the dissolution rate can be calculated. Note that the value of $(C)_{T,b}$, also required for Eq. (45), is a measurable value.

6. RESULTS AND DISCUSSION

To test the ability of the model to predict the dissolution rate in unbuffered and buffered solutions, we attempted to simulate data reported by Mooney and coworkers (7,8). First we simulated the dissolution of 2-naphthoic acid in an unbuffered medium. For the case of 2-naphthoic acid in an unbuffered medium at pH 9, simulated concentration profiles are presented in Fig. 2. All concentration profiles have been normalized so that they can be represented in one graph. Both [HA] and $[A^-]$, the concentration of drug in nonionized and ionized forms, decrease from the surface values to their bulk values (in this case zero). Due to the interaction of chemical reaction and diffusion, their profiles are not straight lines. The concentration of B^- (in this case OH^-) drops from the bulk value and we have higher concentration of H^+ on the surface. The pH of the surface is 4.18, close to the pK_a value of the 2-naphthoic acid, and rises up to pH 9 at the edge of the film. A reaction plane exists at $x = (r - R)/R = 0.92$ where the reactants HA and B^- meet each other and their concentrations drop to equilibrium values.

Figure 3 shows the relationship of the pH at the drug surface to the bulk pH for three weak acids, indomethacin, 2-naphthoic acid, and benzoic acid. The surface pH is predicted to be lower than the bulk pH except when the bulk pH is considerably lower than the drug pK_a. There is a plateau region at a bulk pH greater than the drug pK_a over which the surface pH appears to be dictated by the drug

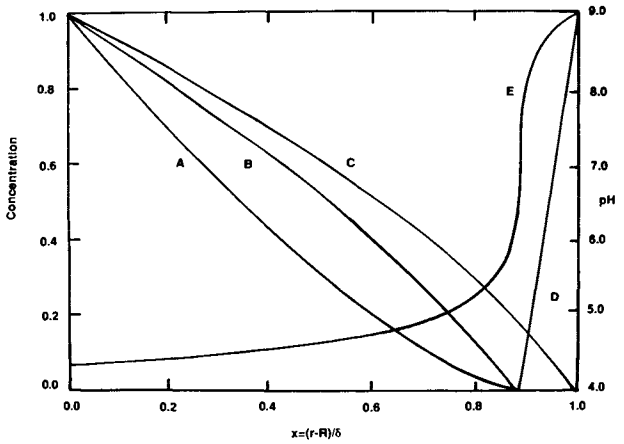

Fig. 2. Fractional concentration profiles with the fractional dimensionless distance across the film for the dissolution of 2-naphthoic acid in a solution with pH 9 containing no buffer (A) HA; (B) H^+; (C) A^-; (D) OH^-; (E) pH.

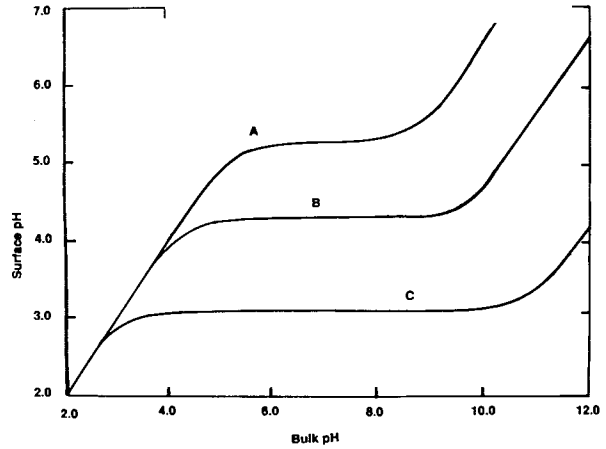

Fig. 3. The relationship between bulk and surface pH's for different weak acids in unbuffered media. (A) Indomethacin; (B) 2-naphthoic acid; (C) benzoic acid.

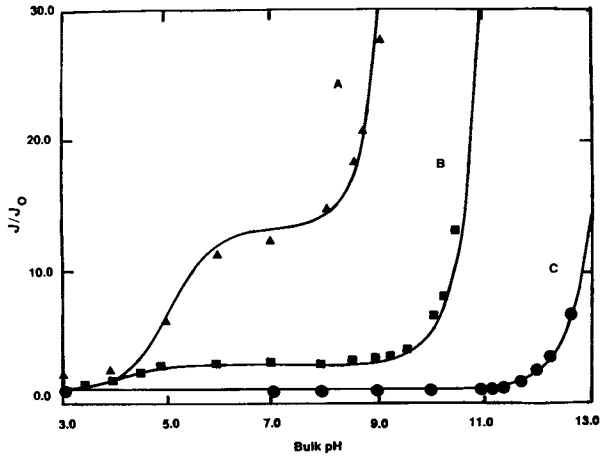

Fig. 4. Relative dissolution rates versus bulk pH for several carboxylic acids at 25°C from a rotating disk at 450 rpm. Experimental data are from Ref. 7 and the solid lines are the model predictions. (▲) Indomethacin; (■) 2-naphthoic acid; (●) benzoic acid.

rather than the bulk pH. At a bulk pH much higher than the drug pK_a, the surface pH rises in proportion to the bulk pH but is considerably lower for any given bulk pH. The ability of a dissolving acid to suppress the surface pH to a value lower than the bulk pH is predicted to depend on its pK_a and solubility. Values for the drugs used in simulations are presented in Table IV. The pH and the width of the plateau are affected by the product of the intrinsic solubility and pK_a as seen from Table II.

The changes in surface pH with bulk pH are directly reflected in the dissolution rates of these compounds. In Fig. 4, simulated rates of dissolution normalized to the intrinsic (pH $\ll$ pK_a) rate for the three compounds in unbuffered media are compared with the experimental data of Mooney and co-workers (7) at various bulk pH levels. An excellent agreement between predicted and experimental values is obtained. Comparison of the shape of the curves in Figs. 3 and 4 clearly illustrates that the key parameter to calculation of the dissolution rate at any given bulk pH is the surface pH value. The failure of dissolution rate to increase proportionately with bulk pH above pK_a has also been noted by Shek (3). Our simulations show that this deviation from dissolution rate predictions based on the total solubility method (2) can be completely accounted for by the discrepancy between the surface and the bulk pH.

The diffusivity ratio in these equations (γ_{HA} and γ_{Bs}) is expected to be very close to unity and we can therefore make approximations as follows:

(i) for acidic drug

$$(C)_{T,s} \simeq [HA]_0\left(1 + \frac{K_a}{[H^+]_s}\right) \tag{51}$$

(ii) and similarly for basic drug

$$(C)_{T,s} \simeq [Bs]_0\left(1 + \frac{[H^+]_s}{K_a}\right) \tag{52}$$

These are analogous to the total solubilities used in the total solubility method (2) but they are based on the surface pH values rather than the pH in the bulk. Since these values may differ greatly, as illustrated in Table V for 2-naphthoic acid in the presence of imidazole base, the prediction of total solubilities and therefore of the dissolution rates from bulk pH's can lead to substantial errors. To indicate the magnitude of the discrepancy, we calculated the solubilities by using the bulk and the actual surface pH's. The error in the conventional total solubility method was 296% for unbuffered solution and 31.8% for a buffer concentration of 0.5 *M* at a bulk pH of 5. For a bulk pH of 9, these deviations were $4.4 \cdot 10^6$ and 3881%, respectively. Only when the bulk pH is very close to or below the drug pK_a are the surface and bulk pH values similar. However, the use of buffer tends to suppress the pH changes and it is clear that the deviation from bulk pH becomes much smaller as the concentration of the buffer increases.

The concentration profiles for 2-naphthoic acid in the presence of imidazole base are presented in Fig. 5. In this particular case, there is no reaction plane and the surface pH is lowered less by ionization of the drug. This can be attributed to the presence of buffer. The general structure of the profiles are in agreement with our expectations, i.e., high concentrations of HA, A^-, H^+, and BH on the surface, with a gradual decrease to the bulk values at the other side of the film. The pH profile is rather flat due to the buffering effect.

It was found experimentally that an increase in the buffer concentration increases the total solubility and hence the dissolution rate. To check our model in this respect we present the calculations from our model in Fig. 6 for the dissolution of 2-napthoic acid in acetate buffer. The experimental data are taken from Mooney and co-workers (8) and

Table IV. Intrinsic Solubilities and pK_a Values for Benzoic Acid, 2-Naphthoic Acid, and Indomethacin at 25°C (7)

Compound	Intrinsic solubility $[HA]_0$ (*M*)	K_a	pK_a
Benzoic acid	$2.11 \cdot 10^{-2}$	$9.25 \cdot 10^{-5}$	4.03
2-Naphthoic acid	$1.3 \cdot 10^{-4}$	$9.64 \cdot 10^{-5}$	4.02
Indomethacin	$2.62 \cdot 10^{-6}$	$6.70 \cdot 10^{-5}$	4.17

Table V. Effect of the Buffer Concentration on the Surface pH for 2-Naphthoic Acid in the Presence of Imidazole Base

	pH, surface, at buffer concentration (*M*)			
pH, bulk	0	0.05	0.10	0.50
2.5	2.5	2.5	2.5	2.5
3	3	3	3	3
3.5	3.48	3.48	3.48	3.48
4	3.87	3.88	3.89	3.92
4.5	4.07	4.13	4.18	4.36
5	4.14	4.38	4.53	4.84
5.5	4.16	4.78	4.99	5.34
6	4.17	5.24	5.47	5.83
6.5	4.17	5.69	5.92	6.29
7	4.17	6.05	6.29	6.70
7.5	4.18	6.28	6.52	6.98
8	4.18	6.39	6.64	7.12
8.5	4.18	6.43	6.68	7.18
9	4.18	6.44	6.69	7.20
9.5	4.19	6.45	6.70	7.20

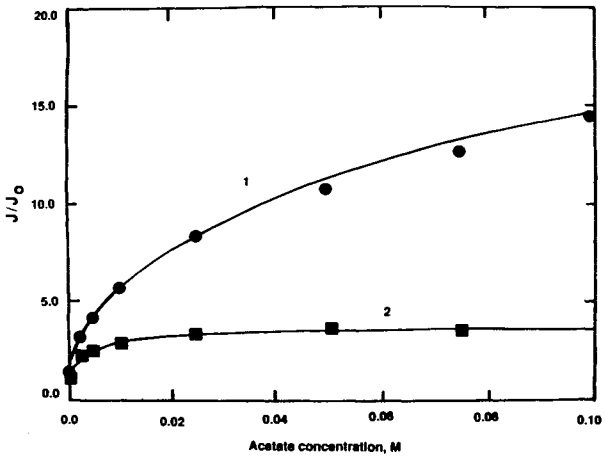

Fig. 6. Relative dissolution rate of 2-naphthoic acid from a solid rotating disk rotating at 450 rpm into media with different concentration of acetate concentration. Line 1, pH 6; line 2, pH 5. The solid lines are the calculated values, and experimental data are from Ref. 8.

a fit of the data equally good to that of the previous authors is obtained. Depending on the bulk pH, the effect of the buffer concentration levels off after a certain concentration. The advantage of the current approach is that the dissolution rates can be directly calculated from the concentration of drug at the surface. This is a function of the hydrogen ion concentration, for which we present an analytical method for calculation (Sections 3.1.4 and 4.4).

There has been some controversy in the literature concerning the effect of the buffer acidity pK_b. The linearity between the dissolution rate and the pK_b suggested to Spitael *et al.* (20) that a Bronsted catalysis influences drug dissolution. Shek (3) questioned this idea by relating the dissolution rate to the buffer capacity of the basic salts in the microenvironment. The current model treats the base conjugate of the buffer (B^-) as a reactant whose relative concentration is determined by the pK_b. As this value increases the fraction of $[B^-]$ increases, leading to a higher total solubility and dissolution rate. In the same context, for a given pK_b, the higher the buffer concentration is, the higher $[B^-]$ and hence the higher the dissolution rate. Figure 7 shows that there is a linar dependence of dissolution rate on buffer pK_b. The buffer concentration (C_B) dependence is also linear in this particular case. It therefore appears unnecessary to invoke a catalysis mechanism to explain the observed results.

7. CONCLUSIONS

In this paper we present a model for drug dissolution from solid drug. It is shown that the dissolution rate is dependent on several parameters. These parameters include the medium (K_b and C_b) and drug (pK_a, $[HA]_0$) properties and the mass transfer characteristics (D and δ) of the system. The model should be useful in prediction of the dissolution rate and complete dissolution time. As the solution is in an accessible form requiring only the solution of second- and

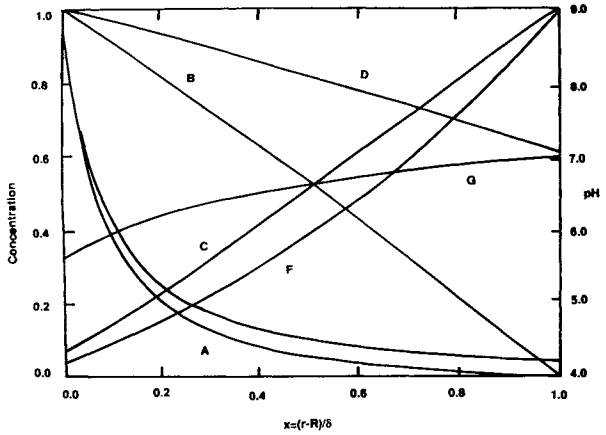

Fig. 5. Fractional concentration profiles with the fractional dimensionless distance across the film for the dissolution of 2-napthoic acid in a solution with pH 7 containing imidazole as buffer. (A) HA; (B) A^-; (C) HB; (D) B^-; (E) H^+; (F) OH^-; (G) pH.

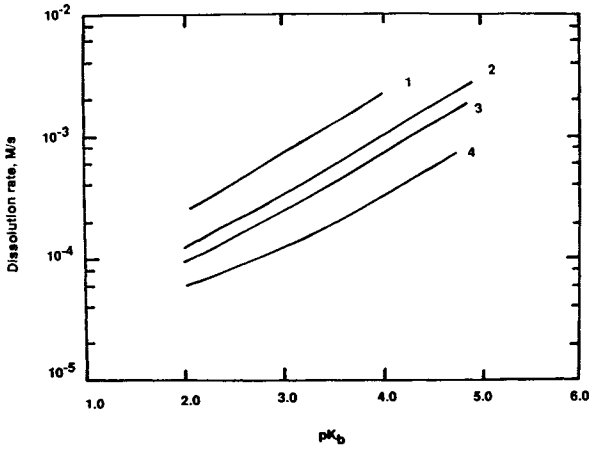

Fig. 7. Effect of buffer concentration and pK_b on the dissolution rate predicted from the model presented. Line 1, C_b = 0.5 *M*; line 2, C_b = 0.1 *M*; line 3, C_b = 0.05 *M*; line 4, C_b = 0.01 *M*.

third-order polynomial equations to calculate the surface pH and subsequently the surface concentrations driving the drug dissolution, it should be useful for the routine prediction of pH and buffer effects on the dissolution behavior of ionizable drugs.

APPENDIX

Example: Calculations for Benzoic Acid at pH 13

To illustrate the calculation procedure for drug surface concentrations we present this example. Here we use the following physical properties: $K_a = 9.33 \cdot 10^{-5}$ M ($pK_a = 4.03$), intrinsic solubility $[HA]_0 = 0.0216$ M, and diffusivities $D_{HA} = D_{A^-} = 9.6 \cdot 10^{-6}$ cm²/sec and $D_{H^+} = D_{OH^-} = 2.7 \cdot 10^{-5}$ cm²/sec (7).

Calculations are done assuming sink conditions in the bulk, i.e., $[HA]_b = [A^-]_b = 0$. From the data $[H^+]_b = 10^{-13}$, then $[OH^-]_b = K_w/[H^+]_b = 10^{-1}$ and the diffusivity ratios $\gamma_1 = D_{OH^-}/D_{H^+} = 1$ and $\gamma_2 = D_{A^-}/D_{H^+} = 0.36$, then the constants in Table II can be calculated as $b = 0.10$ and $c = 7.26 \cdot 10^{-7}$. The conditions at the surface are then computed as $[H^+]_s = 7.256 \cdot 10^{-6}$ or $(pH)_s = 5.14$, and using the equilibrium relationships, Eq. (26), we obtain $[A^-]_s = 0.278$ M and $[OH^-]_s = 1.378 \cdot 10^{-9}$ M. The dynamic total concentration of benzoic acid at the surface is $[HA]_{T,s} = 0.2993$ M.

Note that the pH at the surface is much lower than the bulk pH, illustrating the ability of benzoic acid to buffer the solution layer adjacent to the dissolving solid.

Example: Calculations for Papaverine at pH 2

Here we use the following physical properties: acidity $K_a = 3.63 \cdot 10^{-7}$, intrinsic solubility $[B_s]_0 = 3.08 \cdot 10^{-5}$ M, and diffusivities $D_{Bs} = D_{BsH^+} = 6.8 \cdot 10^{-6}$ cm/sec and $D_{H^+} = D_{OH^-} = 2.7 \cdot 10^{-5}$ cm/sec.

Calculations are done assuming sink conditions, i.e., $[Bs]_b = [BsH^+]_b = 0$. From the data $[H^+]_b = 10^{-2}$, then $[OH^-]_b = K_w/[H^+]_b = 10^{-12}$ and the diffusivity ratios $\gamma_1 = D_{OH^-}/D_{H^+} = 1$ and $\gamma_2 = D_{BsH^+}/D_{H^+} = 0.25$, then the constants in Table II are $a = 8.06 \cdot 10^{-6}$, $b = -3.63 \cdot 10^{-9}$, and $c = 3.63 \cdot 10^{-21}$. The conditions at the surface are calculated as $[H^+]_s = 4.50 \cdot 10^{-4}$ or $(pH)_s = 3.35$, and then using the equilibrium relationships, we get $[BsH^+]_s = [Bs]_0[H^+]_s/K_a = 0.038$ M and $[OH^-]_s = K_w/[OH^-] = 2.22 \cdot 10^{-11}$ M. The dynamic total concentration of drug at the surface is $[Bs]_{T,s} = 0.0382$ M.

Example: Calculations for 2-Naphthoic Acid in Imidazole Base Buffer at pH 9

To illustrate the calculation procedure for drug surface concentrations we present a simple example. Here we use the following physical properties: $K_a = 9.55 \cdot 10^{-5}$ ($pK_a = 4.02$) M, intrinsic solubility $[HA]_0 = 1.3 \cdot 10^{-4}$ M, buffer acidity $K_b = 6.76 \cdot 10^{-8}$ ($pK_b = 7.17$), buffer concentration $C_b = 0.01$ M, and the diffusivities $D_{HA} = D_{A^-} = 9.6 \cdot 10^{-6}$ cm²/sec, $D_{H^+} = D_{OH^-} = 2.7 \cdot 10^{-5}$ cm²/sec, and $D_{HB} = D_{B^-} = 8.20 \cdot 10^{-6}$ cm²/sec (8).

Calculations are done with sink conditions, i.e., $[HA]_b = [A^-]_b = 0$. From the data $[H^+]_b = 10^{-9}$ and $[OH^-]_b = K_w/[H^+]_b = 10^{-5}$. For buffer species, using the equilibirium relationships we get $[B^-]_b = C_bK_b/([H^+]_b + K_b) = 9.85 \cdot 10^{-3}$ and $[HB]_b = C_b - [B^-]_b = 1.46 \cdot 10^{-4}$. The diffusivity ratios $\gamma_1 = 1$, $\gamma_2 = 0.36$, $\gamma_3 = 0.30$, and $\gamma_{HA} = \gamma_{HB} = 1$.

The dynamic total concentrations for buffer and drug in the bulk are $[HB]_{T,b} = [HB]_b + \gamma_{HB}[B^-]_b = 0.01$ and $[HA]_{T,b} = [HA]_b + \gamma_{HA}[A^-]_b = 0$. Then the constants in Table III can be evaluated as $G = -2.965 \cdot 10^{-3}$, $a = 2.965 \cdot 10^{-3}$, $b = -4.47 \cdot 10^{-9}$, $c = -3.02 \cdot 10^{-16}$, $Q = -9.789 \cdot 10^{-7}$, $R = -9.685 \cdot 10^{-10}$, and $\theta = \cos^{-1}(R/\sqrt{Q^3}) = 3.14$ gives $[H^+]_s = 1.57 \cdot 10^{-6}$, or $(pH)_s = 5.80$, and then using the equilibrium relationships at the surface we get $[A^-]_s = K_a[HA]_0/[H^+]_s = 7.90 \cdot 10^{-3}$ M, $[OH^-]_s = K_w/[H^+]_s = 6.37 \cdot 10^{-9}$ M, and $[B^-]_s = K_b[HB]_{T,b}/(\gamma_{HB}K_b + [H^+]_s) = 4.13 \cdot 10^{-4}$. The dynamic total concentration of drug is calculated as $[HA]_{T,s} = 8.03 \cdot 10^{-3}$ M.

NOMENCLATURE

a, b, c, d, e	Polynomial constants
A	Stoichiometric coefficient matrix
A^-	Acid drug, ionized
B^-	Base conjugate of buffer
Bs	Base drug, nonionized
BsH^+	Base drug, ionized
C	Concentration
C	Concentration matrix
$C_1, C_2, \ldots, C_6$	Integration constants
D	Diffusion coefficient
HA	Acid drug, nonionized
HB	Base conjugate of buffer
J	Dissolution flux
K_a	Acidic dissociation constant for drug
K_b	Acidic dissociation constant for buffer
K_w	Equlibrium constant for water
k_s	Mass transfer coefficient
m	Mass
n	Number of moles
r	Radial coordinate
R	Radius
t	Time
t_c	Time for complete dissolution
v	Velocity
x	Dimensionless coordinate, $(r - R)/R$
X	Chemical species, general

Greek

δ	Film thickness
γ_1	Diffusivity ratio, D_{OH^-}/D_{H^+}
γ_2	Diffusivity ratio, D_{A^-}/D_{H^+}, for acids
	Diffusivity ratio, D_{BsH^+}/D_{H^+}, for base
$\gamma_{HA}, \gamma_{HB}, \gamma_{Bs}$	Diffusivity ratios
ρ	Density
ρ_M	Molal density
ϕ	Reaction rate
∇	Gradient operator
∇^2	Laplace operator
ν	Kinematic viscosity
ν	Stoichiometric coefficient
ω	Angular velocity

Subscripts

b	Bulk
0	Initial value (for distances, e.g., R)
	Intrinsic solubility (for concentrations)
s	Surface
T	Total

REFERENCES

1. W. Nernst. *Z. Phys. Chem.* 47:52–55 (1904).
2. A. Goldberg, In L. J. Leeson and J. T. Carstensen (eds.), *Dissolution Technology,* Industrial Pharmaceutical Technology Section, APhA Academy of Pharmaceutical Science, Washington, D.C., 1974.
3. E. Shek. *Pharm. Ind.* 40:981–984 (1978).
4. E. Brunner. *Z. Phys. Chem.* 47:56–102 (1904).
5. W. I. Higuchi, L. Parrott, D. E. Wurster, and T. Higuchi. *J. Am. Pharm. Assoc. Sci. Ed.* 47:376–383 (1958).
6. W. I. Higuchi, E. Nelson, and J. G. Wagner. *J. Pharm. Sci.* 53:333–335 (1964).
7. K. G. Mooney, M. A. Mintun, K. J. Himmelstein, and V. J. Stella. *J. Pharm. Sci.* 70:13–21 (1981).
8. K. G. Mooney, M. A. Mintun, K. J. Himmelstein, and V. J. Stella. *J. Pharm. Sci.* 70:22–32 (1981).
9. J. G. Aunins, M. Z. Southard, R. A. Myers, K. J. Himmelstein, and V. J. Stella. *J. Pharm. Sci.* 74:1305–1316 (1985).
10. J. B. Dressman and D. Fleisher. *J. Pharm. Sci.* 75:109–116 (1986).
11. W. Nernst and E. Brunner. *J. Am. Chem. Soc.* 47:52–102 (1904).
12. A. W. Hixson and J. H. Crowell. *Ind. Eng. Chem.* 23:923–931 (1931).
13. R. B. Bird, W. E. Stewart, and E. N. Lightfoot. *Transport Phenomena,* John Wiley and Sons, New York, 1960.
14. J. Crank. *Mathematics of Diffusion,* University Press, Oxford, 1975.
15. B. O. Palsson. In S. Siedeman and B. Bexar (eds.), *Electrochemical Activation, Metabolism and Perfusion of the Heart Simulation and Experimental Models,* Martinus Nijhoff, Wordrech/Boston/Lancaster, 1986.
16. R. Aris. *The Mathematical Theory of Diffusion and Reaction in Permeable Catalysts,* University Press, Oxford, 1975.
17. C. G. Hill, Jr. *An Introduction to Chemical Engineering Kinetics and Reactor Design,* John Wiley and Sons, New York, 1977.
18. T. K. Sherwood, R. L. Pigford, and C. R. Wilke. *Mass Transfer,* McGraw–Hill, New York, 1975.
19. V. G. Levich. *Physico-chemical Hydrodynamics,* Prentice-Hall, Englewood Cliffs, NJ, 1962.
20. J. Spitael, R. Kinget, and K. Naessens. *Pharm. Ind.* 42:846–849 (1980).
21. B. Carnahan, H. A. Luther, and J. O. Wilkes. *Applied Numerical Methods,* Wiley, New York, 1969.